The effect of fillers on the vibration welding of poly(butylene terephthalate)*

Vijay K. Stokes
GE Corporate Research and Development, PO Box 8, Schenectady, NY 12301, USA
(Received 13 October 1992; revised 15 January 1993)

Two particulate-filled grades of poly(butylene terephthalate) (PBT) containing about 10 and 30 wt% mineral fillers, one particulate-filled polyester blend containing about 65 wt% mineral filler, and two glass-filled grades of PBT containing about 15 and 30 wt% glass fibres have been studied to assess the effects of fillers on the strength of vibration welded butt joints. The weldability of these materials has been characterized at weld frequencies of 120 and 250 Hz and weld pressures of 0.9 and 3.45 MPa. Each of these five materials is shown to exhibit the four phases of vibration welding that are common in unfilled resins. Welds of these five materials are shown to achieve strengths on the order of 89, 58, 85, 69 and 60% of the strengths of the base (filled) resins.

(Keywords: weld strength; fillers; poly(butylene terephthalate))

INTRODUCTION

In vibration welding of thermoplastics, frictional work done by vibrating two parts under pressure, along their common interface, is used to generate heat to effect welds[1]. Past work[1-4] has focused on characterizing the effects of weld parameters, such as the weld frequency, the weld amplitude, the weld pressure and the weld time, on the vibration welding process and the strength of welds for several different thermoplastics. However, except for one study on the effects of glass fillers[5], weld studies to date have been limited to neat resins. This paper systematically examines the effects of particulate and chopped-glass fillers on the weld process and weld strength.

A typical vibration weld for a thermoplastic polymer has four phases[1,2], as shown schematically in *Figure 1*. In the first phase, Coulomb friction generates heat at the interface, raising its temperature to the point at which the polymer can undergo viscous flow. In the second phase, the interface begins to melt and the mechanism of heat generation changes from solid Coulomb friction to viscous dissipation in the molten polymer. The molten polymer begins to flow in a lateral direction, resulting in an increase in the weld penetration — the distance by which the parts approach each other as a result of lateral flow. In the third phase, the melting and flow are at a steady state, and the weld penetration increases linearly with time. When the machine is shut off, the penetration continues to increase because the weld pressure causes the molten film to flow until it solidifies; this is the fourth phase. The welding of dissimilar materials[6-8], chopped-glass-filled materials[5] and structural foams[9] also exhibits these four phases.

The most important parameter affecting the static strength of welds is the penetration. Static weld strengths equal to that of the resin can be achieved when the penetration exceeds a critical threshold — the penetration at the beginning of the steady-state phase — and the strength drops off for penetrations below this value[3,4]. This threshold is affected by the thickness of the part being welded: the threshold increases with part thickness[10]. Additional penetration into the steady-state phase does not affect the weld strength in neat resins[3,4], in blends[4,11], in glass-filled modified poly(phenylene oxide)[5] and in structural foams[9]; however, the strength of welds between dissimilar materials can continue to increase[6-8].

The literature on the welding of particulate-filled and glass-filled thermoplastics is quite small and is mainly concerned with hot-tool welding[12,13]. Bucknall *et al.*[12] presented limited data on the hot-tool welding of polypropylene (PP) containing 40 wt% calcium carbonate, PP containing 20 wt% short glass fibres, and poly(ether sulfone) containing 30 wt% short glass fibres.

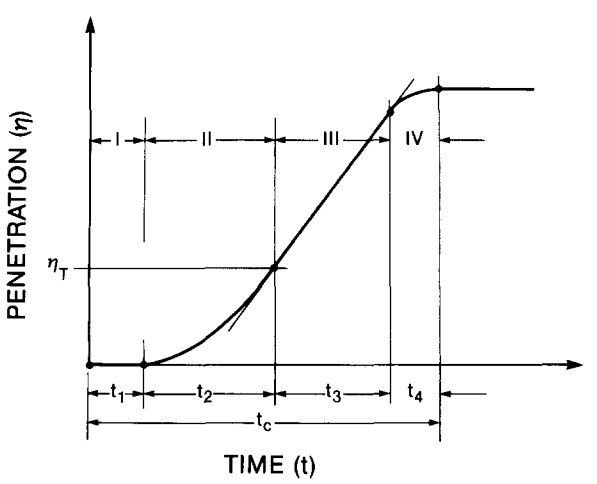

Figure 1 Schematic penetration–time curve showing the four phases of vibration welding

* Based on a paper presented at the Society of Plastics Engineers 51st Annual Technical Conference, 9–13 May 1993, New Orleans, Louisiana, USA

0032-3861/93/214445-10

They reported relative strengths (ratio of the weld strength to the material strength) on the order of 50 and 55% for the calcium-carbonate-filled and glass-filled PP grades, respectively. Andrews and Bevis[13] investigated the hot-tool welding of chopped-graphite-fibre-filled poly(vinylidene fluoride) (PVDF) to itself and to neat, unfilled PVDF. Their investigation, which included a characterization of the fibre-length distribution in the moulded material used for the welding tests, showed that the weld strength of the filled material was significantly lower than the strength of the filled material. The strength of filled to unfilled material joints could, however, be almost as high as that of the unfilled material.

For the same filler and matrix, the effect of fillers on weld strength can be characterized by the weight per cent of filler, the index of filler content that is normally available for commercial filled resins. But if two fillers have very different densities, then, for the same weight per cent filler content, the effective surface area of the fillers with the same geometric characteristics will be very different. In such cases, volume per cent filler content may be a more appropriate measure. Of course, when the filler particles have different shapes, e.g. spherical particles, ellipsoidal particles, flakes or fibres, percentage filler content will not be an adequate discriminator, and some mesure of shape (such as 'aspect ratio') must also be specified.

This paper discusses the vibration welding of two particulate-filled and two glass-filled grades of commercially available poly(butylene terephthalate) (PBT), and a particulate-filled grade of a polyester blend (PEB). The five grades studied are: (1) 10-PF-PBT (VALOX* 744), containing about 10 wt% mineral filler; (2) 30-PF-PBT (VALOX 740), containing about 30 wt% mineral filler; (3) 65-PF-PEB (VALOX HV7065), a polyester blend containing about 65 wt% mineral filler; (4) 15-GF-PBT (VALOX DR51), containing about 15 wt% of chopped glass fibres; (5) 30-GF-PBT (VALOX 420), containing about 30 wt% glass fibres. The volume fraction, v_f, of fillers in a filled material is given by:

$$v_f = 1 - (1 - m_f)\rho_c/\rho_m$$

where m_f is the weight fraction (wt%) and ρ_c and ρ_m are the specific gravities of, respectively, the filled (composite) and matrix materials. Since commercial materials contain many proprietary additives, the matrix density ρ_m is not available. But for estimating the volume per cent filler content, a representative specific gravity of PBT is adequate; a specific gravity of $\rho_m = 1.31$ (VALOX 310) will be used. Then, by using the published values of 1.36, 1.48, 2.40, 1.41 and 1.53 of the specific gravities, estimates for the volume per cent filler contents of 10-PF-PBT, 30-PF-PBT, 65-PF-PEB, 15-GF-PBT and 30-GF-PBT are, respectively, 6.5, 21, 36, 8.5, and 18.

TEST PROCEDURE

Eight specimens were cut from 152 mm x 203 mm injection-moulded plaques, all of which, except the 65-PF-PEB plaques, were gated at the 152 mm edge (gate A in *Figure 2*), according to the layout shown in *Figure 2*. The 65-PF-PEB plaques were gated at the 203 mm edge (gate B in *Figure 2*). The thicknesses of the particulate- and glass-filled plaques were 6.35 and 6.1 mm, respectively. The edges of each specimen were machined to obtain rectangular blocks of size 76.2 mm x 25.4 mm x thickness, thereby assuring accurate alignment of surfaces during butt welding. The specimens were individually numbered according to the scheme shown. Welds were conducted on sets of mating specimens from the same plaque. In this way it was possible to track variations across plaques due to varying both filler distributions and fibre orientations.

Fibre orientation in the specimens, which depends on both the location in the specimen and its thickness, was not characterized. However, for purposes of comparison, four 152 mm x 25.4 mm specimens, corresponding to locations 1–4 in *Figure 2*, were cut from the 152 mm x 203 mm plaques. These specimens were subjected to the same strength tests as the welded specimens, thereby providing a basis for evaluating the strengths of welded joints.

Details of the weld procedure are described in reference 3. Two specimens with machined lateral edges are vibration welded along 2.54 mm x thickness edges

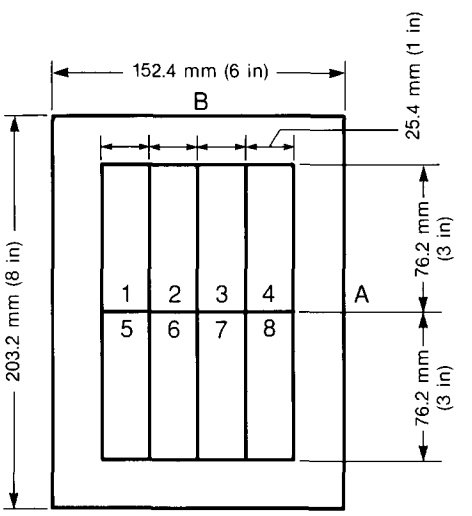

Figure 2 Layout showing locations of eight numbered specimens cut from 152 mm x 203 mm injection-moulded plaques

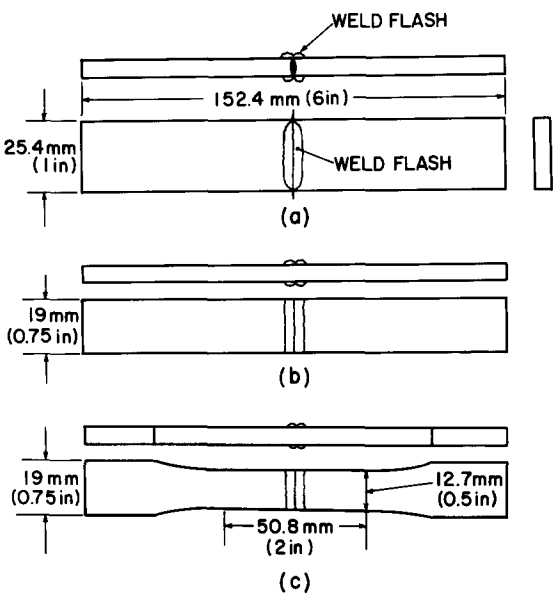

Figure 3 Specimens for determining the weld strength of butt welds

* VALOX is a registered trademark of the General Electric Company

resulting in a bar with dimensions 152.4 mm × 25.4 mm × thickness, which is then routed down to a standard ASTM D638 tensile test specimen with the vibration-welded butt joint in its centre, as shown in *Figure 3*. These bars are then subjected to a constant displacement rate tensile test corresponding to a nominal strain rate of $10^{-2}\,s^{-1}$. During each strength test, the average strain across the weld interface is measured with an extensometer of gauge length 25.4 mm. Because of the local nature of failure, this extensometer only establishes the lower limit of the strain at failure; the actual strain can be much higher in many cases.

PENETRATION–TIME DATA

Representative penetration–time curves for the two particulate-filled grades of PBT and one particulate-filled grade of PEB, for a frequency of $n = 120$ Hz, a weld amplitude of $a = 1.59$ mm, and two weld pressures of $p_0 = 0.9$ and 3.45 MPa, are shown in *Figure 4*. Clearly, they exhibit the four phases of vibration welding, shown schematically in *Figure 1*, that have been observed in neat resins[1], blends[4,11], structural foams[9] and a glass-filled resin[5]. The intersections of these curves with the thin horizontal line show where the vibratory motion was stopped (initiation of phase IV) at a penetration of 0.51 mm. Beyond this point the molten film continues to flow while being cooled to a solid phase, resulting in an additional penetration, η_c. As expected, higher pressures result in shorter cycle times. Increasing the filler content from 10 to 30 wt% results in an increase in the cycle time. But the cycle times for the PEB containing 65 wt% mineral filler are substantially shorter; this must reflect differences between the rheology of PBT and PEB, differences in the densities and shapes of the mineral fillers used and, possibly, other additives in these materials.

The penetration, η_T, at which the steady state initiates, the steady-state penetration rate, $\dot{\eta}$, and the phase IV penetration increment, η_c, for each of the six tests shown in *Figure 4* are listed in *Table 1*. The table also includes data for straight PBT[4]. The differences between the penetration rates for 10-PF-PBT and 30-PF-PBT are quite small; the penetration rates appear to be comparable to those for PBT. As expected, the penetration rate increases with the pressure. Also, the

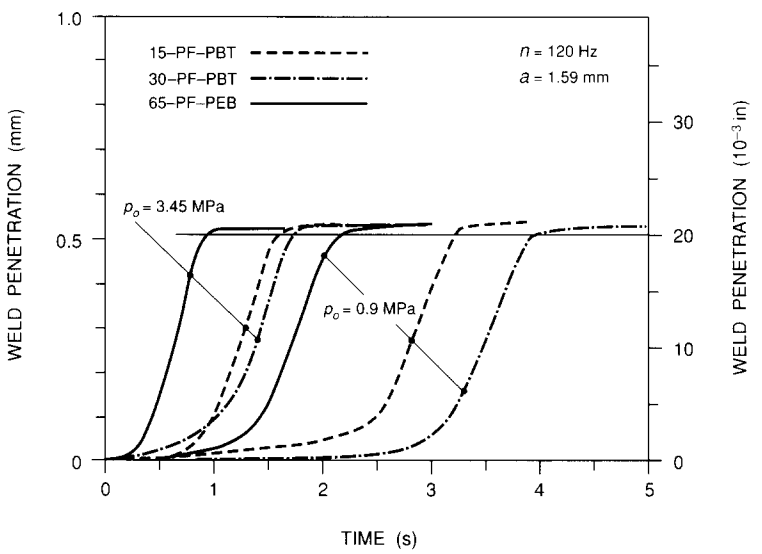

Figure 4 Penetration–time curves for particulate-filled PBT and PEB for $n = 120$ Hz, $a = 1.59$ mm and $p_0 = 0.9$ and 3.45 MPa

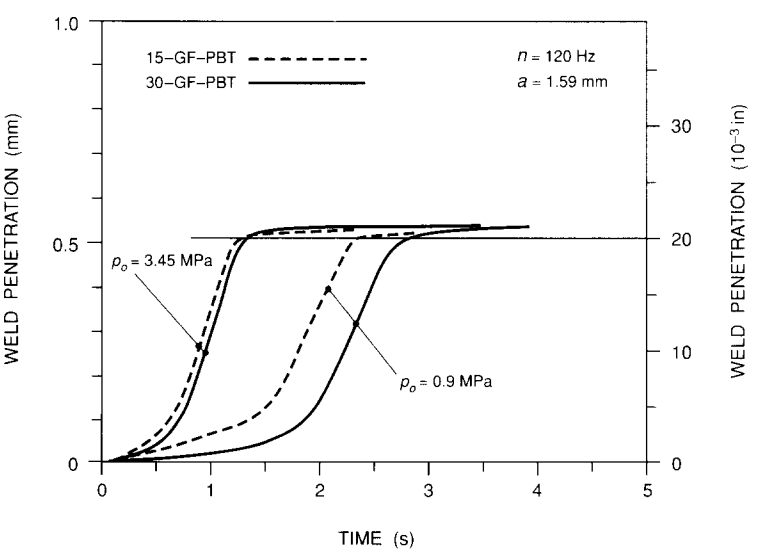

Figure 5 Penetration–time curves for glass-filled PBT for $n = 120$ Hz, $a = 1.59$ mm and $p_0 = 0.9$ and 3.45 MPa

values of η_c are a little smaller for the material with the lower filler content, but both are smaller than for the straight PBT. The penetration rates for the 65-PF-PEB are larger than for PBT, probably reflecting differences in the rheology of PBT and PEB, and η_c is lower than for the other two materials. All in all, although the filler content does affect the cycle time, it has a surprisingly small effect on the penetration rate.

Penetration–time curves for the two glass-filled grades of PBT are shown in *Figure 5* (for the same process conditions as in *Figure 4*). As in the particulate-filled materials, the cycle time increases with the glass content. The corresponding data in *Table 1* indicate that the penetration rates for these two materials are comparable. The penetration rates for these glass-filled materials are a little lower than for the particulate-filled materials at the lower pressure of 0.6 MPa. However, for $p_0 = 3.45$ MPa, the penetration rates for all but the 65-PF-PEB grade are the same as that for straight PBT.

WELD STRENGTHS OF PARTICULATE-FILLED PBT AND PEB

Weld strengths of 10-PF-PBT, 30-PF-PBT and 65-PF-PEB are listed, respectively, in *Tables 2–4* for $n = 120$ Hz and $a = 1.59$ mm, and for $n = 250$ Hz and $a = 0.44$ mm, at two weld pressures of $p_0 = 0.9$ and 3.45 MPa. *Table 2* also lists data for 120 Hz welds of 10-PF-PBT at a weld pressure of 0.52 MPa. In these tests, the vibratory weld motion was stopped (end of phase III) at penetrations of $\eta_0 = 0.25$ and 0.51 mm. Because the molten film continues to flow outward during phase IV, the final penetration η_F is somewhat larger than these values; the excess corresponds to the incremental penetration $\eta_c = \eta_F - \eta_0$ during phase IV, which is on the order of 0.02–0.05 mm. The symbol t_0 in these tables represents the time during which the specimens were vibrated (from start to end of phase III), and is a measure of the cycle time. The relative weld strength σ_w/σ_u is the ratio of the actual weld strength, σ_w, to the strength σ_u of the filled material. The value of σ_u was obtained by tests on tensile bars cut from the four locations 1–4 on plaques shown in *Figure 2*. The values of σ_u obtained from these four locations were quite consistent for the 10-PF-PBT and 30-PF-PBT, but there was somewhat more scatter in the four values for 65-PF-PEB; the mean values for each material are reported at the bottom of the corresponding table together with values of the strain to failure, ε_0. The strain at the failure across the weld, ε_w, measured by an extensometer with gauge length 25.4 mm, is also listed. The actual locations from which weld pairs were obtained are also give in the tables.

Table 1 Penetration at the initiation of the steady-state phase, steady-state penetration rate and the phase IV penetration for 120 Hz welds of five filled grades of PBT at a weld amplitude of 1.59 mm at two weld pressures

Material	p_0 (MPa)	η_T (mm)	$\dot{\eta}$ (mm s^{-1})	η_c (mm)
10-PF-PBT	0.9	0.23	0.62	0.04
10-PF-PBT	3.45	0.18	0.76	0.04
30-PF-PBT	0.9	0.16	0.60	0.05
30-PF-PBT	3.45	0.23	0.79	0.05
65-PF-PEB	0.9	0.17	0.67	0.02
65-PF-PEB	3.45	0.15	0.93	0.02
15-GF-PBT	0.9	0.19	0.57	0.04
15-GF-PBT	3.45	0.19	0.76	0.02
30-GF-PBT	0.9	0.17	0.54	0.05
30-GF-PBT	3.45	0.19	0.77	0.03
PBT	0.9	0.13	0.69	0.06
PBT	3.45	0.38	0.76	0.05

Table 2 Strength and ductility data for 120 and 250 Hz welds of 6.35 mm thick 10-PF-PBT at a strain rate of $\dot{\varepsilon} = 0.01$ s^{-1}

n (Hz)	a (mm)	p_0 (MPa)	η_F (mm)	t_0 (s)	σ_w (MPa)	σ_w/σ_u	ε_w (%)	Specimen pairs
120	1.59	0.52	0.32	4.51	39.3	0.62	1.36	(2, 6)
120	1.59	0.52	0.33	4.69	49.2	0.79	1.88	(1, 5)
120	1.59	0.52	0.57	4.43	48.4	0.77	1.89	(4, 8)
120	1.59	0.52	0.58	4.59	59.2	0.94	2.63	(3, 7)
120	1.59	0.9	0.30	2.78	55.0	0.87	2.11	(1, 5)
120	1.59	0.9	0.32	3.57	46.1	0.73	1.84	(1, 5)
120	1.59	0.9	0.53	2.90	55.6	0.88	2.34	(3, 7)
120	1.59	0.9	0.56	3.23	56.3	0.89	2.29	(3, 7)
120	1.59	3.45	0.29	1.14	54.7	0.87	2.23	(2, 6)
120	1.59	3.45	0.30	1.53	53.7	0.85	2.14	(2, 6)
120	1.59	3.45	0.53	1.43	53.5	0.85	2.09	(4, 8)
120	1.59	3.45	0.55	1.61	53.6	0.85	2.02	(4, 8)
250	0.44	0.9	0.56	8.83	53.2	0.84	2.28	(1, 5)
250	0.44	0.9	0.56	7.26	51.2	0.81	1.97	(2, 6)
250	0.44	3.45	0.55	4.02	51.0	0.81	2.09	(3, 7)
250	0.44	3.45	0.55	3.96	48.5	0.77	1.92	(4, 8)

$\sigma_u = 63.2$ MPa, $\varepsilon_0 = 3.9\%$

Table 3 Strength and ductility data for 120 and 250 Hz welds of 6.35 mm thick 30-PF-PBT at a strain rate of $\dot{\varepsilon} = 0.01$ s^{-1}

n (Hz)	a (mm)	p_0 (MPa)	η_F (mm)	t_0 (s)	σ_w (MPa)	σ_w/σ_u	ε_w (%)	Specimen pairs
120	1.59	0.9	0.30	3.75	20.5	0.39	0.50	(1, 5)
120	1.59	0.9	0.32	4.49	17.4	0.33	0.41	(1, 5)
120	1.59	0.9	0.55	3.92	29.4	0.56	0.74	(3, 7)
120	1.59	0.9	0.56	4.80	29.3	0.56	0.76	(3, 7)
120	1.59	3.45	0.30	1.82	28.6	0.54	0.76	(2, 6)
120	1.59	3.45	0.30	2.09	27.4	0.52	0.75	(2, 6)
120	1.59	3.45	0.55	1.75	30.4	0.58	0.82	(4, 8)
120	1.59	3.45	0.56	2.22	30.7	0.58	0.83	(4, 8)
250	0.44	0.9	0.55	10.83	32.5	0.62	0.90	(1, 5)
250	0.44	0.9	0.55	8.22	32.0	0.61	0.82	(2, 6)
250	0.44	3.45	0.55	5.96	32.0	0.61	0.83	(3, 7)
250	0.44	3.45	0.55	5.20	32.0	0.61	0.80	(4, 8)

$\sigma_u = 52.7$ MPa, $\varepsilon_0 = 2.63\%$

Table 4 Strength and ductility data for 120 and 250 Hz welds of 6.35 mm thick 65-PF-PEB at a strain rate of $\dot{\varepsilon} = 0.01$ s^{-1}

n (Hz)	a (mm)	p_0 (MPa)	η_F (mm)	t_0 (s)	σ_w (MPa)	σ_w/σ_u	ε_w (%)	Specimen pairs
120	1.59	0.9	0.30	2.18	33.7	0.73	0.51	(1, 5)
120	1.59	0.9	0.30	2.22	33.7	0.73	0.51	(1, 5)
120	1.59	0.9	0.53	2.16	36.6	0.80	0.55	(3, 7)
120	1.59	0.9	0.53	2.13	35.5	0.77	0.53	(3, 7)
120	1.59	3.45	0.29	0.70	39.1	0.85	0.54	(2, 6)
120	1.59	3.45	0.29	0.75	39.8	0.87	0.61	(2, 6)
120	1.59	3.45	0.53	0.96	38.4	0.84	0.57	(4, 8)
250	0.44	0.9	0.53	5.04	34.2	0.74	0.52	(1, 5)
250	0.44	0.9	0.55	4.92	33.9	0.74	0.53	(2, 6)
250	0.44	3.45	0.53	2.06	37.0	0.81	0.57	(3, 7)
250	0.44	3.45	0.53	2.16	36.8	0.80	0.54	(4, 8)

$\sigma_u = 46.0$ MPa, $\varepsilon_0 = 0.74\%$

The data in *Table 2* show that welds of 10-PF-PBT (10 wt%, 6.5 vol% filler content) can achieve relative strengths on the order of 90% for 120 Hz welds and 85% for 250 Hz welds. On the basis of these limited data, it would appear that optimal weld strength is achieved at weld pressures between 0.52 and 0.9 MPa. The mean failure strain across the weld (actual strains can be expected to be higher) of $\varepsilon_w = 2.29$ ($\sigma_w/\sigma_u \approx 0.9$) gives a relative failure strain of $\varepsilon_w/\varepsilon_0 = 0.59$.

The results in *Table 3* show that relative weld strengths on the order of 0.6 can be obtained in 30-PF-PBT (30 wt%, 21 vol% filler content), representing a substantial reduction from the weld strengths attainable for 10-PF-PBT. For 120 Hz welds, the strength appears to improve with the pressure; relative strengths of 0.58 can be obtained. The strengths of 250 Hz welds are somewhat higher at $\sigma_w/\sigma_u \approx 0.61$, and do not appear to be as sensitive to weld pressure. Using a value of $\varepsilon_w = 0.83$ gives $\varepsilon_w/\varepsilon_0 = 0.35$, indicating the large embrittling effect of the higher filler content ($\varepsilon_w/\varepsilon_0 = 0.59$ for 10-PF-PBT).

The data in *Table 4* show that slightly higher weld strengths can be achieved in 65-PF-PEB at the lower weld frequency of 120 Hz — relative strength of about 0.85 at 120 Hz *versus* 0.8 at 250 Hz. (Some of the differences may not be very significant because of more scatter in the properties of this material: four tensile bars showed $\sigma_u = 51, 47, 40, 45$ MPa with $\varepsilon_0 = 0.87, 0.82, 0.59, 0.68$, respectively.) Given the high particulate loading (65 wt%, 36 vol%), these relative strengths are surprisingly high (compare with 30-PF-PBT: 30 wt%, 21 vol%), but may reflect differences in the matrix resin and in the densities and shapes of the particulate fillers. A value of $\varepsilon_w = 0.55$ gives $\varepsilon_w/\varepsilon_0 = 0.74$, which is even higher than for 10-PF-PBT.

The strength data for these three particulate-filled resins are compared in *Figure 6*, which shows the relative strength *versus* the penetration for $n = 120$ Hz (open symbols) and $n = 250$ Hz (solid symbols) at different pressures. The decrease in the relative weld strength of 30-PF-PBT in comparison to that of 10-PF-PBT is understandable in view of the large differences in filler content. But the high relative weld strength of 65-PF-PEB is rather surprising: the filler content (65 wt%, 36 vol%) is much higher than that of 30-PF-PBT (30 wt%, 21 vol%). This surprisingly high strength must reflect the rheology of the resins (PEB *versus* PBT), the additives and the types of particulate fillers used. Using the published specific gravities of the three particulate-filled materials and a matrix specific gravity of 1.31, estimates for the specific gravities of the fillers in 10-PF-PBT, 30-PF-PBT and 65-PF-PEB are 2.1, 2.1 and 4.4, respectively. Thus the particulate filler in 65-PF-PEB is very different from those in the other two materials; the shapes of the particles may also be different.

Scanning electron microscopy (SEM) was used to study the effects of the particle–resin morphology on weld strength. Three specimens of 30-PF-PBT were chosen for this purpose: (a) the fracture surface of a tensile test specimen (unwelded); (b) the fracture surface of a high-strength weld made at 120 Hz at a weld pressure of 3.45 MPa (see data in row 8 in *Table 3*); and (c) the fracture surface of a high-strength weld made at 250 Hz at a weld pressure of 0.9 MPa (see data in row 10 in *Table 3*). The SEM micrographs are shown in two groups of three corresponding, respectively, to these three specimens. Each set of figures shows the three surfaces at one magnification: *Figures 7a–c* show these three fracture surfaces at a magnification of 100×. Note the very rough fracture surface of the unwelded specimen (*Figure 7a*). The fracture surfaces of the welded specimens, both of

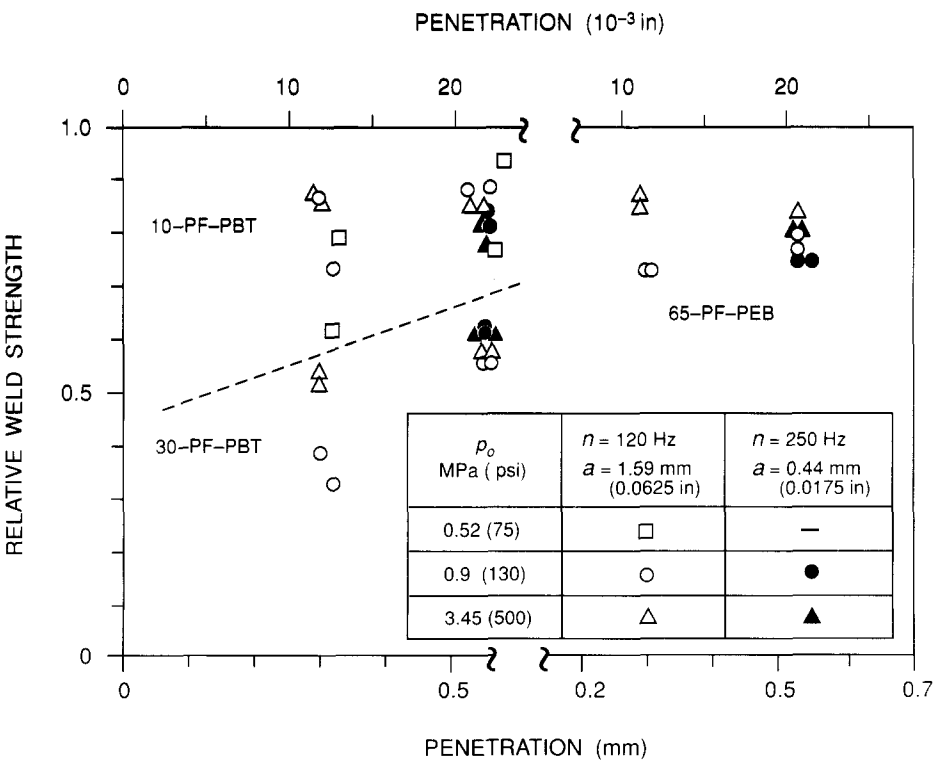

Figure 6 Relative strength *versus* penetration for 120 and 250 Hz welds of particulate-filled PBT and PEB at two weld pressures

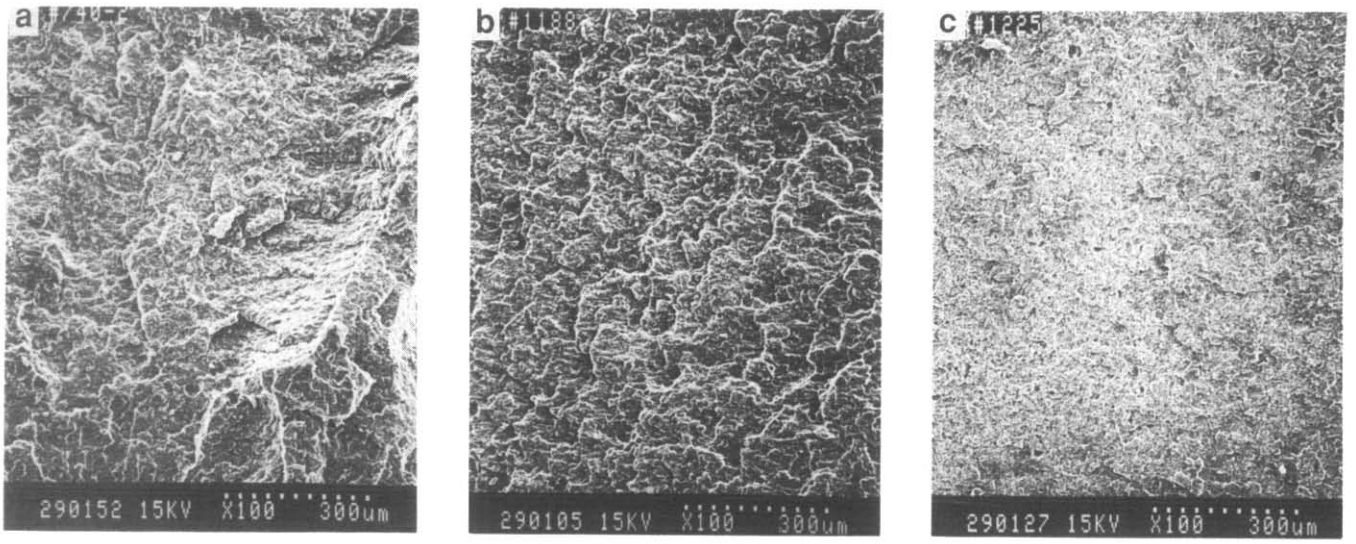

Figure 7 SEM micrographs (original magnification 100×) of the fracture surfaces of three 30-PF-PBT specimens: (a) unwelded specimen; (b) specimen welded at 120 Hz at a weld pressure of 3.45 MPa; (c) specimen welded at 250 Hz at a weld pressure of 0.9 MPa

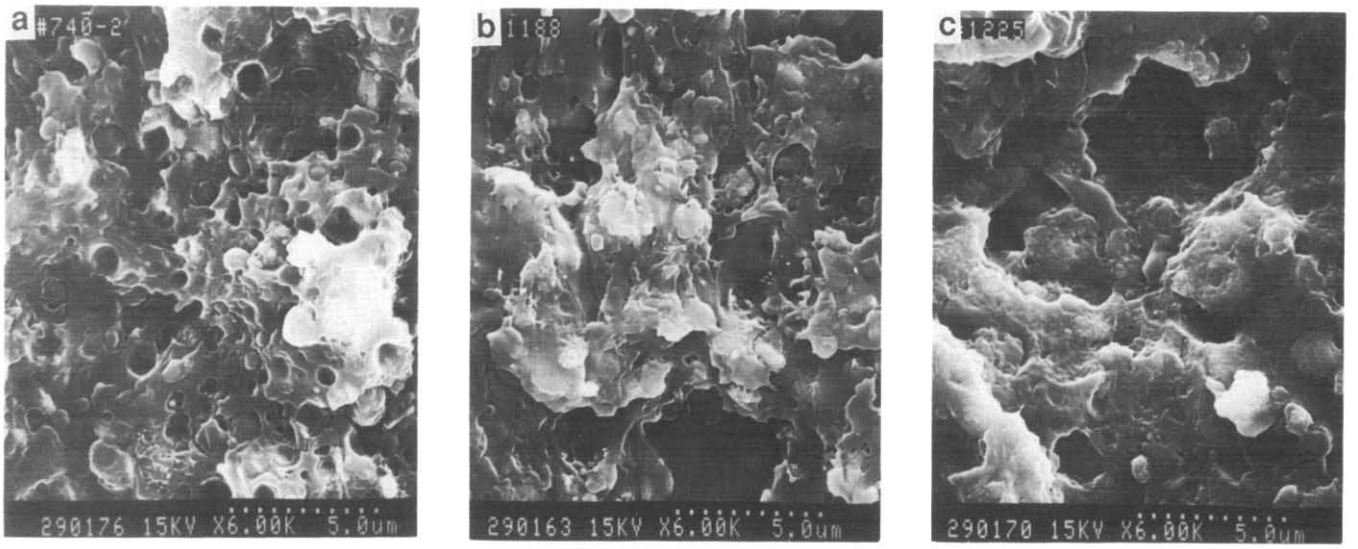

Figure 8 SEM micrographs (original magnification 6000×) of the fracture surfaces of the three 30-PF-PBT specimens shown in *Figure 7*

which failed at the weld interface, are planar; the lower frequency, higher pressure welds (*Figure 7b*) exhibit a rougher fracture surface than the higher frequency, lower pressure welds (*Figure 7c*). Pits on the fracture surface of the unwelded specimen, from which particles have been pulled out, can be seen in great abundance in 1000× SEM micrographs (not shown); this morphology is quite different from that of the two weld surfaces in which such pits cannot be seen. Higher magnification SEM micrographs (6000× in *Figure 8*) not only show these pits in the fracture surface of the unwelded specimen, but also clearly show particles embedded in the matrix. Note that these particles are heavily coated with resin. Pits are difficult to discern in the fracture surfaces of the two welded specimens (*Figures 8b, c*), although resin-coated particles can be seen, especially in the high frequency, low pressure welds (*Figure 8c*).

WELD STRENGTH OF GLASS-FILLED PBT

Weld strength data for 15-GF-PBT and 30-GF-PBT are listed, respectively, in *Tables 5* and *6* (the data are for the same process conditions as for the particulate-filled materials.) These two tables have an additional column listing values of σ_w/σ_u^*, where σ_u^* is the tensile strength measured on a bar from the same location as the welded bar. For example, the weld strength of the pair (3, 7) is normalized by the tensile strength of a bar from location 3 (see *Figure 2*). This is an attempt to account for fibre orientation effects; however, it is a rather crude attempt because failure at the weakest point in a tensile specimen may not correspond to the fibre distribution in the same specimens at the weld interface location. However, a comparison of σ_w/σ_u with σ_w/σ_u^* does give an indication of the amount of scatter that may be expected in the weld strength data.

The data in *Table 5* show that relative weld strengths on the order of 0.68 can be achieved in 15-GF-PBT with $\varepsilon_w/\varepsilon_0 \approx 0.6$ ($\varepsilon_0 = 1.45$). Comparable weld strengths can be attained at both weld frequencies. For 30-GF-PBT (*Table 6*), although relative weld strengths on the order of 0.6 can be achieved at 120 Hz, the relative strengths at 250 Hz are consistently lower at $\sigma_w/\sigma_u \approx 0.52$. For this material, $\varepsilon_0 \approx 1\%$ implies $\varepsilon_w/\varepsilon_0 \approx 0.21$. Thus, while the

relative weld strengths of 15-GF-PBT and 30-GF-PBT are reduced to about 0.68 and 0.6, respectively, the reductions of the relative strains to 0.6 and 0.21, respectively, indicate a more dramatic reduction in the ductility of the weld.

The strength data for both these glass-filled grades of PBT are compared in *Figure 9*, which shows the relative strength *versus* the penetration for $n = 120$ Hz (open symbols) and $n = 250$ Hz (solid symbols) at two pressures. Given the large difference in the amount of glass, the rather small difference in the attainable relative weld strength (0.68 *versus* 0.6) is surprising. The results for these two glass-filled grades of PBT are in line with the relative weld strength of 0.71 obtained for a 20 wt% glass-filled grade of modified poly(phenylene oxide)[5].

For the glass-filled material, SEM was used to study the differences between the fracture surfaces of (a) an unwelded tensile test specimen, and (b) 120 Hz weld made at a pressure of 3.45 MPa (see data in row 7 in *Table 6*) of 30-GF-PBT material. The micrographs are shown in *Figures 10–12*; each figure shows the morphology of (a) the unwelded, and (b) the welded fracture surface at one magnification. The 100 × magnification SEM micrograph in *Figure 10a* shows the irregular fracture surface of an unwelded specimen (the irregularities are more apparent in lower magnification SEMs, which are not shown); large numbers of randomly oriented glass fibres are seen to protrude from the irregular fracture surface. In contrast, the plane surface of the weld failure surface (*Figure 10b*) appears to be

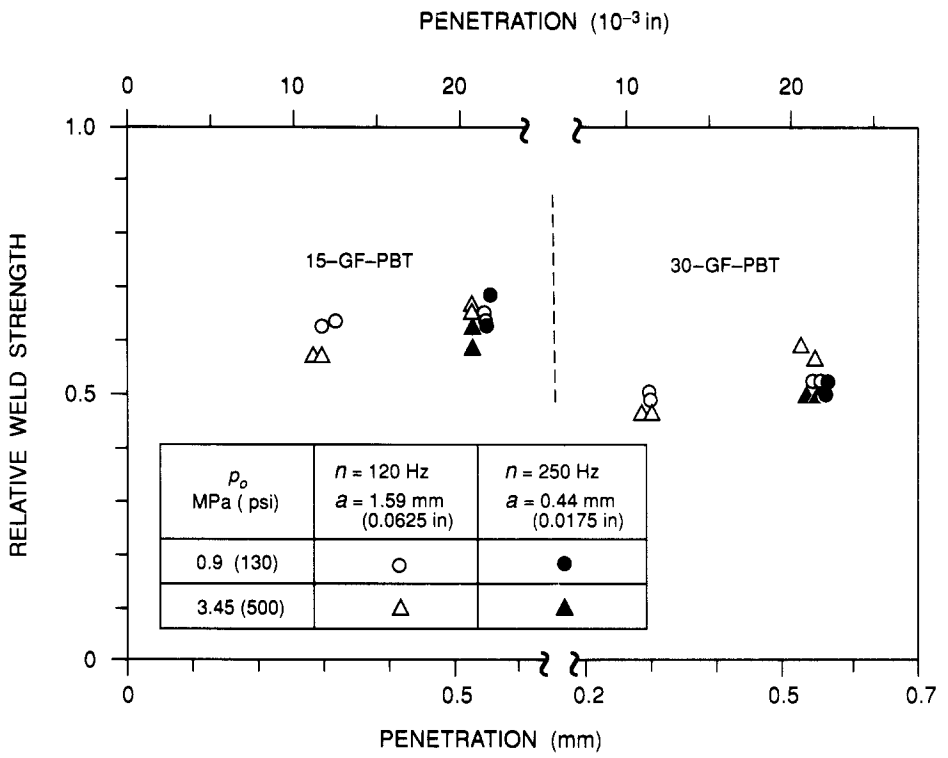

Figure 9 Relative strength *versus* penetration for 120 and 250 Hz welds of glass-filled PBT at two weld pressures

Table 5 Strength and ductility data for 120 and 250 Hz welds of 6.1 mm thick 15-GF-PBT at a strain rate of $\dot{\varepsilon} = 0.01\ s^{-1}$

n (Hz)	a (mm)	p_0 (MPa)	η_F (mm)	t_0 (s)	σ_w (MPa)	$\frac{\sigma_w}{\sigma_u}$	ε_w (%)	Specimen pairs	$\frac{\sigma_w}{\sigma_u^{*a}}$
120	1.59	0.9	0.30	2.03	54.4	0.63	1.17	(1, 5)	0.64
120	1.59	0.9	0.32	2.38	55.1	0.64	1.29	(1, 5)	0.64
120	1.59	0.9	0.55	2.33	55.7	0.64	1.36	(3, 7)	0.65
120	1.59	0.9	0.55	2.48	56.5	0.65	1.43	(3, 7)	0.66
120	1.59	3.45	0.29	0.94	50.0	0.58	1.14	(2, 6)	0.56
120	1.59	3.45	0.30	0.98	50.3	0.58	1.19	(2, 6)	0.57
120	1.59	3.45	0.53	1.28	57.5	0.66	1.38	(4, 8)	0.75
120	1.59	3.45	0.53	1.26	57.9	0.67	1.45	(4, 8)	0.76
250	0.44	0.9	0.55	6.15	54.6	0.63	1.20	(1, 5)	0.64
250	0.44	0.9	0.56	5.68	59.3	0.68	–	(2, 6)	0.67
250	0.44	3.45	0.53	2.56	54.5	0.63	1.27	(3, 7)	0.64
250	0.44	3.45	0.53	2.51	51.2	0.59	1.16	(4, 8)	0.67

$\sigma_u = 86.7$ MPa, $\varepsilon_0 = 2.42\%$

[a] The value of σ_u^* depends on where the specimen was cut from

Table 6 Strength and ductility data for 120 and 250 Hz welds of 6.1 mm thick 30-GF-PBT at a strain rate of $\dot{\varepsilon}=0.01\ s^{-1}$

n (Hz)	a (mm)	p_0 (MPa)	η_F (mm)	t_0 (s)	σ_w (MPa)	$\frac{\sigma_w}{\sigma_u}$	ε_w (%)	Specimen pairs	$\frac{\sigma_w}{\sigma_u^{*a}}$
120	1.59	0.9	0.30	2.69	46.2	0.51	0.82	(1, 5)	0.47
120	1.59	0.9	0.30	2.57	45.2	0.50	0.79	(1, 5)	0.46
120	1.59	0.9	0.55	2.53	47.8	0.53	1.02	(3, 7)	0.53
120	1.59	0.9	0.56	2.73	47.8	0.53	1.00	(3, 7)	0.53
120	1.59	3.45	0.29	1.05	43.0	0.47	0.86	(2, 6)	0.46
120	1.59	3.45	0.30	0.98	43.0	0.47	0.75	(2, 6)	0.46
120	1.59	3.45	0.53	1.32	54.4	0.60	1.01	(4, 8)	0.66
120	1.59	3.45	0.55	1.36	51.4	0.57	0.91	(4, 8)	0.63
250	0.44	0.9	0.56	5.96	46.3	0.51	0.80	(1, 5)	0.48
250	0.44	0.9	0.56	5.83	46.9	0.52	0.83	(2, 6)	0.50
250	0.44	3.45	0.55	2.66	47.4	0.52	0.82	(3, 7)	0.53
250	0.44	3.45	1.33	3.98	45.4	0.50	0.93	(4, 8)	0.55

$\sigma_u=90.6$ MPa, $\varepsilon_0=2.9\%$

[a] The value of σ_u^* depends on where the specimen was cut from

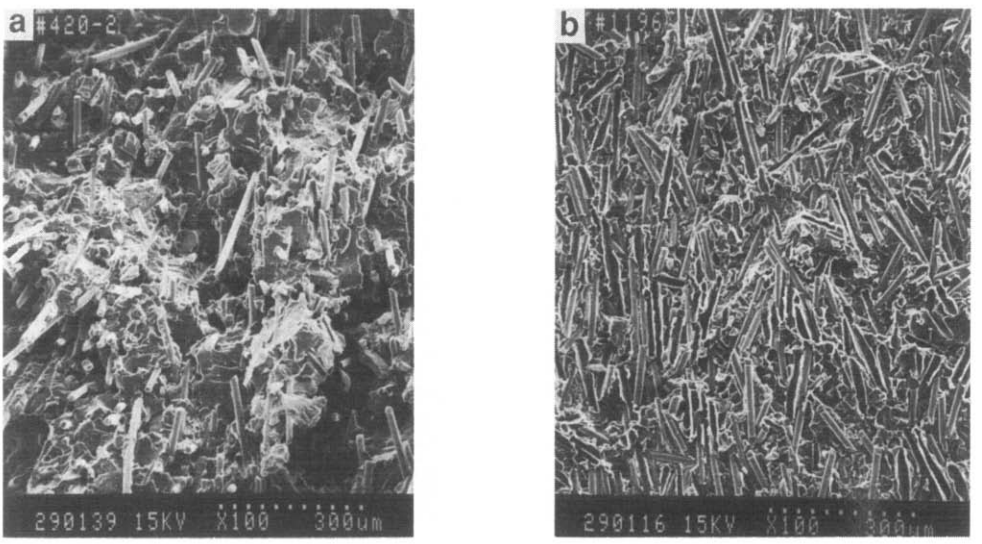

Figure 10 SEM micrographs (original magnification 100×) of the fracture surfaces of two 30-GF-PBT specimens: (a) unwelded specimen; (b) specimen welded at 120 Hz at a weld pressure of 3.45 MPa

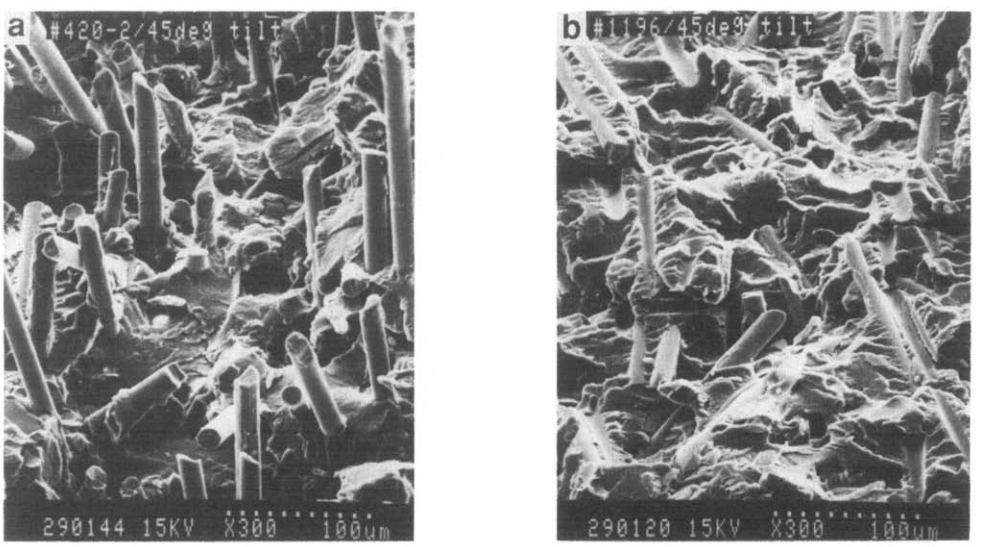

Figure 11 SEM micrographs (original magnification 300×) of the fracture surfaces of the two 30-GF-PBT specimens shown in *Figure 10*. Note 45° tilt of the specimens

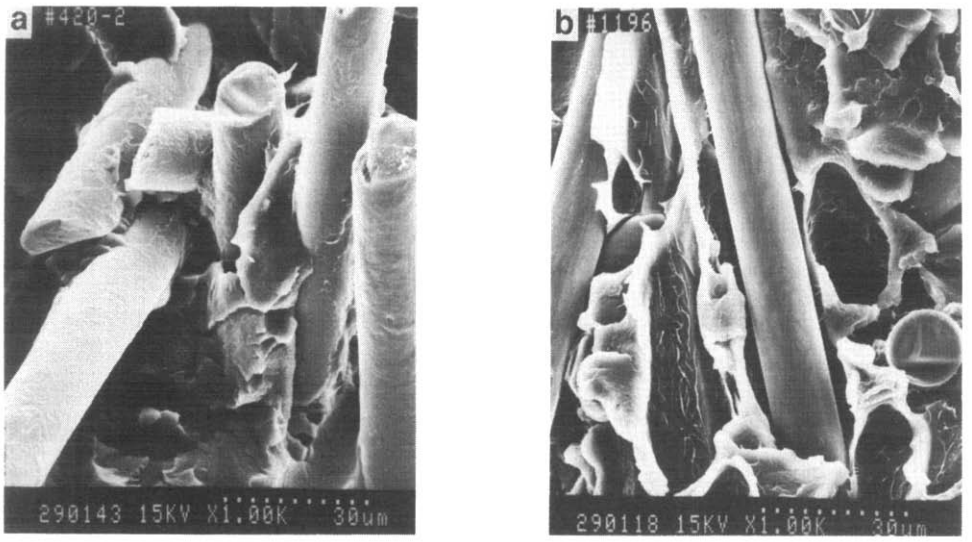

Figure 12 SEM micrographs (original magnification 1000×) of the fracture surfaces of the two 30-GF-PBT specimens shown in *Figure 10*

strewn with fibres aligned along the direction of the vibratory motion. Also, in the unwelded specimen (*Figure 10a*), large numbers of fibres stick out from the matrix, and holes from which the fibres have been pulled out can be seen. But in the welded specimen (*Figure 10b*) the fibres lie mostly in the plane of the interface; there is no evidence of fibre pull-out, but depressions from which fibres in the interface have been pulled out can be seen. The difference between the two surfaces can be seen more clearly from the 300× SEM micrographs in *Figure 11*, in which the specimens are tilted at 45° to show the embedded fibres sticking out in the unwelded specimens. Finally, the 1000× SEM micrographs in *Figure 12* show that while the exposed fibres in the unwelded specimen fracture surface are coated with resin, indicating that failure occurs in the resin, the fibres in the welded specimen fracture surface have little or no resin on their surfaces. Thus, in the welded specimens, the fibres are not well bonded to the matrix and failure occurs at this weak resin–fibre interface.

Thus there are two main causes for strength reduction in glass-filled resins. The intense shear in the molten film in vibration welding orients the fibres along the direction of the vibratory motion. On subsequent solidification, the fibres in the weld zone are frozen mainly in the plane of the weld, with very little bridging across the interface. This is the likely cause for most of the weld strength reduction. Poor bonding between fibres and matrix resin on melting and solidification during welding also contributes to reduced strength. The SEM micrographs in *Figures 10–12* show trends that are similar to those observed in vibration welds of a 20 wt% glass-filled grade of modified poly(phenylene oxide)[5].

CONCLUDING REMARKS

The process phenomenology for the welding of particulate- and glass-filled PBT is clearly similar to that for neat resins: the penetration–time curves exhibit the four phases that are typical for neat resins. In all cases, with all other parameters held constant, the cycle time decreases with an increase in pressure. For the same base resin, the filler content has a remarkably small effect on the steady-state penetration rate. Even the effect on the cycle time appears to be small for the same filler type; however, for the same filler loading, the cycle times are lower for the glass-filled materials.

For the same base resin, increasing filler content reduces the attainable relative weld strength. Although the base strengths of 30-PF-PBT and 30-GF-PBT are very different (52.7 and 90.6 MPa, respectively), their maximum relative weld strengths are remarkably the same, on the order of 0.6. Increase in filler content does decrease the ductility of the weld, i.e. the relative strain at which failure occurs in the weld decreases.

One way of assessing the effect of fillers is to compare the maximum weld strength with that of the base resin. This is not easily done because, in addition to the main filler, filled materials may contain additives that can affect the mechanical behaviour of the base resin and this information is not available for commercial materials. In the absence of more information, the strength of straight PBT may be used as a reference. The strength of this semicrystalline resin can depend on the processing conditions and the location on the plaque from which the test specimen is cut; for PBT (VALOX 310) four bars[4] had strengths of 65.2, 60.1, 61.8 and 58.7 MPa, giving a mean strength of 61.5 MPa. The five filled grades, 10-PF-PBT, 30-PF-PBT, 65-PF-PEB, 15-GF-PBT and 30-GF-PBT, exhibited maximum weld strengths σ_w of 59.2, 32.5, 39.8, 59.3 and 54.4 MPa, respectively. Using the strength $\sigma_r = 61.5$ MPa of PBT as a measure of the strength of the base resin, the strengths of the welds of the filled materials relative to that of the base resin, σ_w/σ_r, are given, respectively, by 0.96, 0.53, 0.65, 0.96 and 0.88. Of these, the result for 65-PF-PEB is the least reliable because the polymer matrix of this material is a blend, so that using the base strength of PBT may not be appropriate. Welds of the 30 wt% mineral-filled PBT are only able to attain about 50% of the strength of the base resin. The relative strengths of the remaining three mineral- and glass-filled grades are remarkably high, on the order of 90–95%. Even the 30 wt% glass-filled grade can attain about 90% of the strength of the base (filled) resin.

ACKNOWLEDGEMENTS

Support provided by GE Plastics is gratefully acknowledged. The contribution of K. R. Conway, who carried out all the tests, is greatly appreciated. Special thanks are due to Julia A. Kinloch for her help and patience during the preparation of this paper.

REFERENCES

1 Stokes, V. K. *Polym. Eng. Sci.* 1988, **28**, 718
2 Stokes, V. K. *Polym. Eng. Sci.* 1988, **28**, 728
3 Stokes, V. K. *Polym. Eng. Sci.* 1988, **28**, 989
4 Stokes, V. K. *Polym. Eng. Sci.* 1988, **28**, 998
5 Stokes, V. K. *Polym. Eng. Sci.* 1991, **31**, 511
6 Stokes, V. K. and Hobbs, S. Y. *Polym. Eng. Sci.* 1989, **29**, 1667
7 Hobbs, S. Y. and Stokes, V. K. *Polym. Eng. Sci.* 1991, **31**, 509
8 Stokes, V. K. and Hobbs, S. Y. *Polymer* 1993, **34**, 1222
9 Stokes, V. K. *J. Mater. Sci.* 1992, **27**, 5073
10 Stokes, V. K. *Polym. Eng. Sci.* 1989, **29**, 1683
11 Stokes, V. K. *Polymer* 1992, **33**, 1237
12 Bucknall, C. B., Drinkwater, I. C. and Smith, G. R. *Polym. Eng. Sci.* 1980, **20**, 432
13 Andrews, J. R. F. and Bevis, M. *J. Mater. Sci.* 1984, **19**, 653